IEEE Journal of Translational Engineering in Health and Medicine

Received 24 November 2017; revised 13 February 2018 and 12 March 2018; accepted 24 March 2018.
Date of publication 8 May 2018; date of current version 25 May 2018.

Digital Object Identifier 10.1109/JTEHM.2018.2822302

A Community-Based IoT Personalized Wireless Healthcare Solution Trial

PHILIP A. CATHERWOOD[1], DAVID STEELE[1], MIKE LITTLE[2], STEPHEN MCCOMB[1], AND JAMES MCLAUGHLIN[1]

[1]NIBEC, Ulster University, Newtownabbey BT37 0QB, U.K.
[2]RFproximity, Belfast BT3 9DT, U.K.

CORRESPONDING AUTHOR: P. A. CATHERWOOD (p.catherwood@ulster.ac.uk)

This work was supported by the InvestNI Connected Health Innovation Centre.

ABSTRACT This paper presents an advanced Internet of Things point-of-care bio-fluid analyzer; a LoRa/Bluetooth-enabled electronic reader for biomedical strip-based diagnostics system for personalized monitoring. We undertake test simulations (technology trial without patient subjects) to demonstrate potential of long-range analysis, using a disposable test 'key' and companion Android app to form a diagnostic platform suitable for remote point-of-care screening for urinary tract infection (UTI). The 868 MHz LoRaWAN-enabled personalized monitor demonstrated sound potential with UTI test results being correctly diagnosed and transmitted to a remote secure cloud server in every case. Tests ranged over distances of 1.1-6.0 Km with radio path losses from 119-141 dB. All tests conducted were correctly and robustly received at the base station and relayed to the secure server for inspection. The UTI test strips were visually inspected for correct diagnosis based on color change and verified as 100% accurate. Results from testing across a number of regions indicate that such an Internet of Things medical solution is a robust and simple way to deliver next generation community-based smart diagnostics and disease management to best benefit patients and clinical staff alike. This significant step can be applied to any type of home or region, particularly those lacking suitable mobile signals, broadband connections, or even landlines. It brings subscription-free long-range bio-telemetry to healthcare providers and offers savings on regular clinician home visits or frequent clinic visits by the chronically ill. This paper highlights practical hurdles in establishing an Internet of Medical Things network, assisting informed deployment of similar future systems.

INDEX TERMS Clinical diagnostics, Internet of Things, LoRa, remote healthcare, sensor networks, urinary Tract Infection.

I. INTRODUCTION

The Internet of Things (IoT) is expected to have a disruptive impact across industry and society, with 20.8 billion IoT connected devices forecast by 2020 [1]. The Internet of Things seeks to inter-connect many physical devices such as vehicles, consumer electronics, buildings, environmental sensors, etc. to facilitate the collection and exchange of data. The IoT market size is predicted to grow from USD 157.05 billion in 2016 to USD 661.74 billion by 2021, a growth driven by the proliferation of smarter and more cost-effective sensors, the emergence of cloud computing, and the maturity and expanse of the high speed internet [2]. Global investment will expedite the propagation of Internet of Things technologies; for example, Chinese manufacturers have asserted that in the coming years they will spend an annual $127b on IoT devices and infrastructure [3].

Significant recent interest in Wireless Sensor networks (the key enabler for IoT-based systems) including developing effect routing protocols, and a range of applications including medical imaging [4], [5]. Further work has been done to explore emerging new and emerging wireless network strategies with an amount of work tackling IoT network developments [6]–[10] and innovations to create smarter IoT networks [11]–[14]. These, as well as cross-application with supporting technologies [15]–[17] helps to generate a range of novel medical applications [18] including imaging [19]–[21] and object detection [22] that address growing societal needs for early cancer detection and

TABLE 1. Comparison of available enabling wireless technologies.

	IoT technology	Frequency of operation (EU/US)	Data rate	Upper operating range	Typical transmit power
[35]	LoRa	868/915MHz	50kbps	25Km	14dBm
[36]	Sigfox	868/915MHz	300bps	50Km	14dBm
[37]	Bluetooth 4	2.4GHz	1Mbps	0.1Km	0/4/10dBm
[38]	Bluetooth 5	2.4GHz	2Mbps (125Kbps for PHY)	0.25Km (0.8Km for PHY)	0/4/10/20dBm
[39]	ZigBee	2.4GHz	250kbps	10-100m	12dBm
[40]	4G	800, 1800, 2600MHz	12Mbps	10Km	23dBm
[41]	5G	Lower bands	3.6Gbps	10Km	23dBm
[41]	5G	Higher bands	10Gbps	<1Km	23dBm
[42]	NB-IoT (NB1)	900MHz	250 kbps	35km	20/23dBm
[43]	Z-Wave Alliance	900MHz	9.6/40/100kbps	30m	0dBm
[44]	Wi-Fi	2.4GHz and 5GHz	802.11(b) 11M; (g) 54M; (n) 0.6, (Gac) 1Gbps	50m	15dBm
[45]	NFC	13.56MHz	100–420kbps	10cm	23dBm (NF)
[46]	EC-GSM	900MHz	140kbps	100Km	20/23dBm
[42]	LTE-M (M1)	700, 1450 - 2200, 5400MHz	0.144Mbps	35km	20/23dBm

developing world healthcare solutions. A key to new remote healthcare devices is in addressing real-world issues with power [23]–[29].

One such enabling IoT technology is LoRa which is the physical layer technology (using a derivative of Chirp Spread Spectrum (CSS) [30] for a Low Power Wide Area Network (LPWAN). LoRa infrastructure has been developed in recent years and its expansion appears to be increasing in rate as more countries choose to deploy full-coverage networks [31]. It operates in the license-free Industrial Scientific and Medical (ISM) radio bands with devices in Europe (as well as Africa, Russia, and Asia) operating at 868 MHz and in USA/Canada at 915 MHz [30], [32]. Three layers of encryption ensure high levels of security; this is particularly significant for the transmission of patient's personal data. With a maximum of 62,500 devices per gateway (dependent on user data rates which can be up to 50 kbps) it allows ubiquitous IoT in urban areas, while its long range (20 Km) makes it ideal for sparsely populated regions [30]. Target sectors include domestic waste management, smart parking, seawater pollution measurement, electricity/water/gas meters, highway tolls, vending machine monitoring, golf course irrigation management, etc. Its key benefits include easy installation, subscription-free service (no mobile SIM card), highly secure two-way communication, long battery life (5-10 years) and low cost [30]. These make it stand apart from other wireless technologies such as cell phone networks. LoRaWAN has been discussed, trialled, and evaluated as an e-Health Communication Technology [33]–[35], however none of the published material discusses using LoRaWAN (or any LPWAN technology) as the basis of a care home or domiciliarypoint-of-care automated test that is transmitted to the cloud.

A comparison of popular IoT technologies (Table 1) highlights such LPWAN technologies as LoRa, NB-IoT, EC-GSM, LTE-M, and Sigfox which boast very low power, low data throughput, highly secure communications, typical device to base-station ranges of 25Km in rural areas and 5 Km in cities [36]–[46]. This technology is coming to fruition at a time when healthcare systems are straining due to an ageing population [47]. IoT-enabled remote healthcare devices can allow patients to return to their homes more quickly after a hospital stay, or to remove the need for a hospital stay altogether. Patients can be monitored from the comfort and familiarity of their own homes and clinicians can respond rapidly to changes in conditions. Telehealth monitoring has been shown to reduce Emergency Room visits by 15%, emergency admissions by 20%, bed days by 14%, tariff costs by 8%, and patient death rates by a remarkable 45% [48]. Telehealth monitoring has also been shown to have predictive value in the study of early detection of heart failure (HF) decompensation events [49].

Remote healthcare has attracted interest for some time [50]; more recently the advancing technology has increased potential for monitoring patients from afar. Smart homes fitted with multitudes of sensors can monitor the chronically ill continuously [51] however such expensive technology is not essential to monitor people at home. IoT facilitated remote health monitoring system has many benefits over customary health monitoring system [52]. IoT devices can be used to enable remote health monitoring of patients with chronic diseases such as cardiovascular diseases (CVD) [53], while long-term Electrocardiogram (ECG) monitoring in residential environments have been proposed [54].

Current challenges demand a profound restructuring of the global healthcare system [55] and the financial viability of such systems has been studied and verified [56] which make the vision of a ubiquitous IoT wireless sensor network for healthcare a valid proposition [57]. Existing IoT solutions for industry are relatively large and cumbersome; to achieve portable and wearable IoT-healthcare devices requires effort to make the hardware less physically intrusive [58]. The use

of IoT technologies to support hospital healthcare and remote monitoring has been presented previously [59]–[61], often taking the form of localized body-centric wireless sensor networks which relay data to an in-house base station which has internet connectivity. LPWAN IoT technologies offer connectivity over extended distances and are also suitable for links where devices are positioned indoors [62]; this has potential to eliminate the need for a domiciliary internet connection, base station, and associated equipment. The trade-off is with regards to the volume of data that can be relayed back to base [63]–[65]. LPWAN techniques include an array of technologies such as Sigfox, LoRa, LTE-M, NB-IoT, etc. LPWAN technology has been presented as a solution to monitor health and wellbeing remotely including portable body-worn monitoring [66]. The LoRa solution is particularly attractive as it requires no mobile network device (and thus no subscription SIM card), nor does it require the home to have Wi-Fi or even a land line.

The presented patient monitoring solution blends both emerging and developed technologies to equip the global healthcare system with medical solutions capable of meeting the growing sector demands. This work is easily scalable and could quickly be utilized to include futuristic medical body-area sensor networks [67]–[70]. Key drivers of this work include the global ageing population [47]; increasing volume of chronic conditions [71]; current international health economics; and the emergence of enabling technologies. The work is supported by the recommendations of [72] who envisage new technology as the key to improvements in healthcare provision, with [73] predicting appropriate implementation of digital technology in the health service could result in efficiency savings up to £10 billion in England alone by 2020.

Recently there has been an amount of work published regarding point-of-care devices. These include the novel use of capacitive touch screens to detect urinary tract infection (UTI) to create a point-of-care device [74], the use of a long-range surface plasmon-polariton (LRSPP) waveguide biosensor for UTI detection [75], the use of Surface enhanced Raman Spectroscopy (SERS) to test for UTIs [76], a number of smartphone-based strip colorimetric detection systems used to remove the subjectivity of results interpretation [77]–[79] (although these are inherently affected by ambient light conditions and require significant post processing), etc.

Other work includes the detection of Urinary Tract Infections on lab-on-chip device by measuring photons emitted from adenosine 5′-triphosphate (ATP) bioluminescence [80], the use of test strips to test for UTIs with a discussion on how an electronic reader (electrochemical sensor array) may be developed [81], and point-of-care tests for Sickle Cell Disease (SCD) [82].

We therefore present the findings of recent development activity to accomplish a remote point-of-care bio-fluid sample analyzer enabled with IoT capability for residential home use. This device employs biomarker detection strips using a transmission-based optical sensing technique and the trial

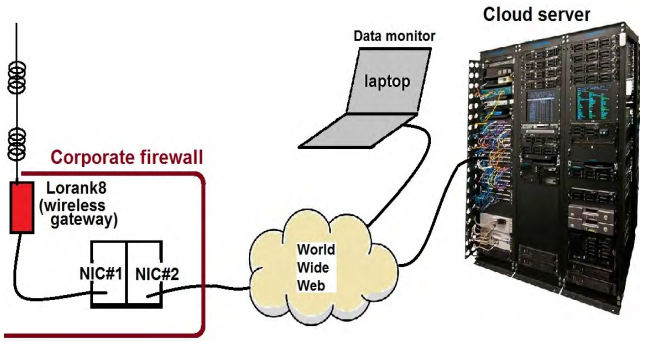

FIGURE 1. Block diagram of the medical LoRa network.

focused on UTI diagnosis, with the results being relayed back to the attending clinician using a long-range IoT network (LoRa) (and simultaneously to the patient via Bluetooth (BLE) to the mobile app. for the patient's benefit). Such a system will save money for the NHS, reduce patient re-admissions, and potentially saves lives [83].

II. EXPERIMENTAL METHODS

A. NETWORK DESIGN

The network was set up as depicted in Fig. 1. The gateway (also known as the base station) that receives data from the medical devices was the Lorank8 from Dutch company Ideetron [84]. Onto this was attached a Sirio GP-901-C 800mm high-gain omnidirectional co-linear antenna ($1/4\lambda + 2 \times 1/2\lambda$ co-linear) with a gain of 5-8.15 dBi at 868 MHz. The gateway was connected to a computer with two Network Interface Controller (NIC) cards via RJ45 Ethernet cable; one NIC card was connected to the internet and the other to the Lorank8 gateway. This allowed the Lorank8 to communicate with the back-end secure cloud server with a fixed Internet Protocol (IP) address so that results appear on the chosen secure server and can either be read directly from the server using a Message Queuing Telemetry Transport (MQTT) client to monitor received traffic on the server (we used a laptop running MQTT.fx software) or forwarded to a visualization service to present the data in a user friendly manner. Use of the MQTT publish-subscribe telemetry protocol allows for bi-directional communication between a MQTT client (PC, computing device, etc.) and a MQTT broker. The MQTT feed presents the payload information from the IoT-enabled bio-device and is displayed in Base-64. This is extracted into a Matlab program for this work and displayed in readable ASCII text.

B. DIAGNOSTIC SYSTEM DETAILS

The diagnostic system uses an emerging IoT platform (LoRa) to transmit the results from the portable point-of-care bio-fluid sample analyzer up to a cloud server (via the Lorank8 gateway). The point-of-care analyzer is an IoT-enabled version of the University's own Qualcomm Tricorder XPRIZE finalist device (''Diagnostic reader'' module

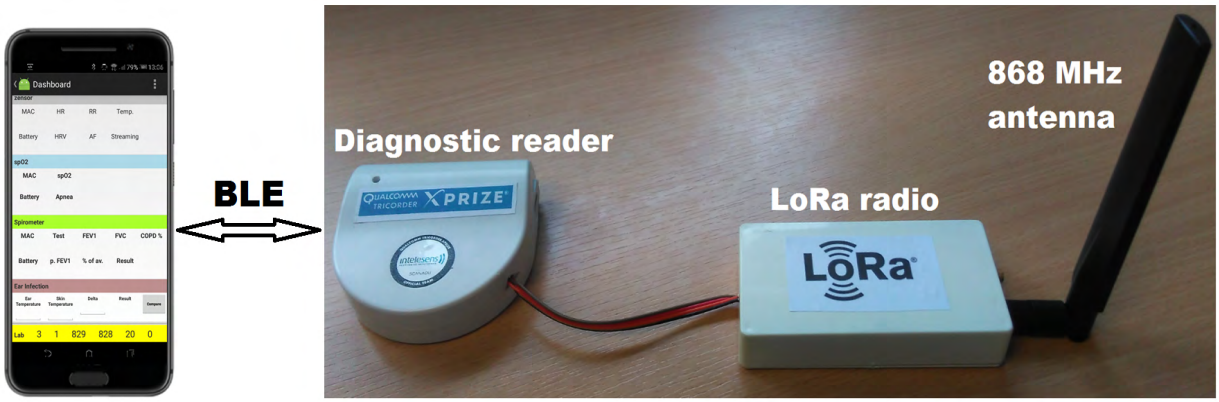

FIGURE 2. Bio-fluid sample tester system with LoRa radio.

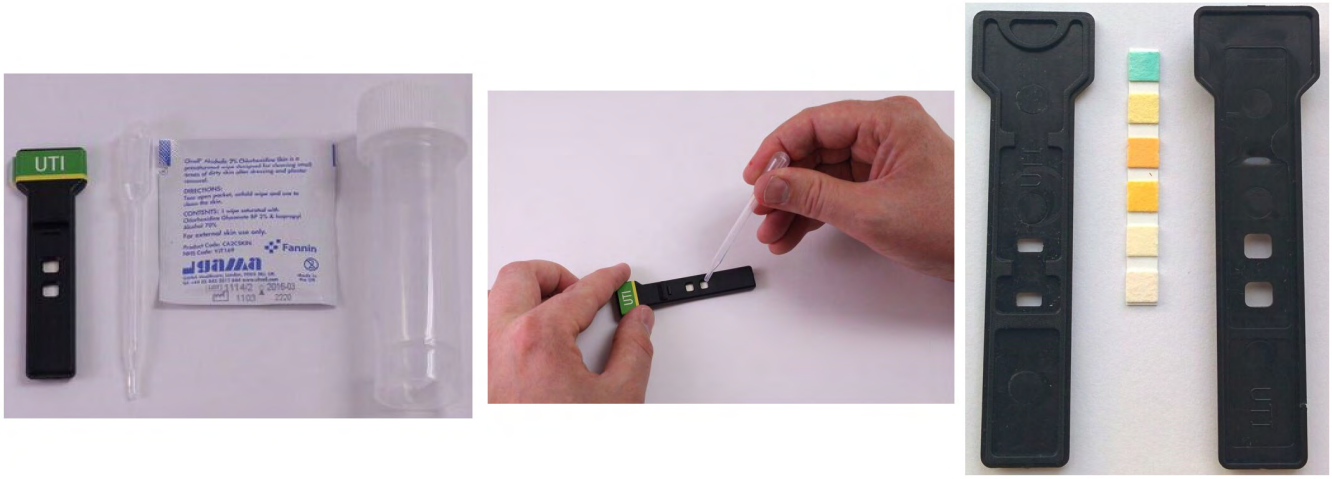

FIGURE 3. Disposable 'key' kit (left), sample being applied to lateral flow 'key' (center), and 'key' composite parts (right).

shown in Fig. 2) [85]. This diagnostic reader uses an optical transmission technique that measures the amount of absorption caused by bio activated gold particles as controlled by a lateral flow geometry or colour changes due to a colorimetric process Absorption profiles relate to qualitative and quantitative measurements of analyses such as nitrate-ions (NIT) or leucocytes (LEU) in UTI's. The diagnostic reader uses a LoRa chip solution (Microchip RN2483) to enable the diagnostic reader to connect to the LoRa IoT network. Such technology could help meet the needs of the global blood pressure devices market (worth US$2b by 2022 [86]), and the global diabetes devices market (worth US$35.5b by 2024 [87]).

The portable LoRa/BLE-enabled electronic diagnostic reader (Fig. 2) is an optical transmission-based system that can be used to obtain both qualitative and quantitative measurements from lateral flow and dipstick tests. The LoRa-enabled diagnostic device, together with a disposable test 'key' (Fig. 3) and companion Android app (depicted in Fig. 2), form a diagnostic platform that is capable of diagnosing multiple medical conditions rapidly; for this trial we emphasize the application of remote healthcare for point-of-care screening of urine samples for evidence of a UTI. A combination of well-defined clinical symptoms, the accessible nature of the urine matrix, and the precedent set by existence of a current (albeit error-prone) point-of-care test make UTI an appropriate use case for demonstration of improved point-of-care diagnostics.

This diagnostics platform is however not limited to UTI diagnosis. More complex pathological conditions are also amenable to analysis. For these, a lateral-flow, antibody-based biomarker detection approach has been implemented, whereby labelled, biomarker-specific antibodies react with patient sample before being detected through accumulation of colored label on a detection membrane located in-line with the optical transmission system. From a user-perspective the mode of operation and associated costs are similar. Fig. 4 outlines the process flow for the system and highlights how the test result is communicated to both the mobile app via BLE and to the securer sever via LoRa radio. The main

IEEE Journal of Translational Engineering in Health and Medicine

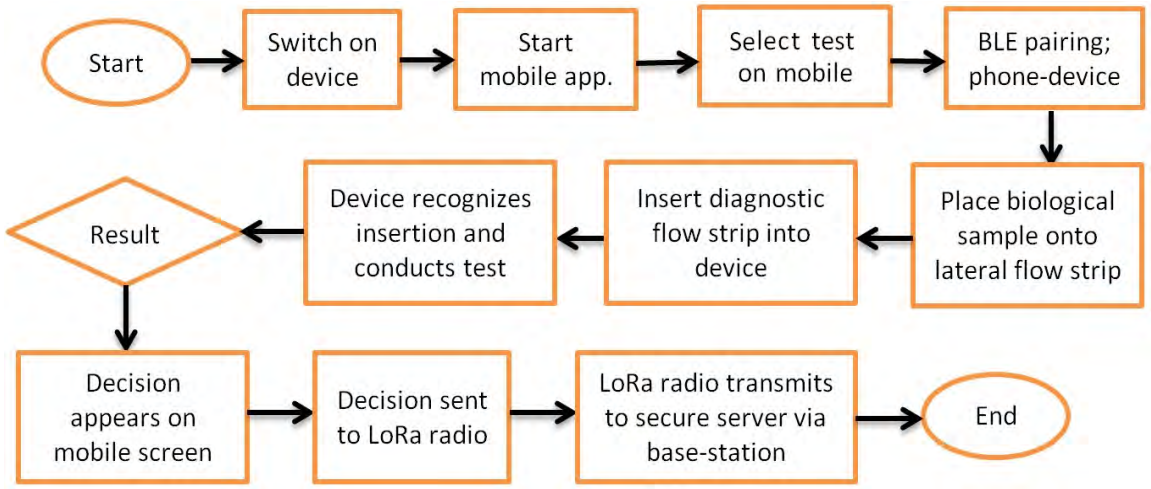

FIGURE 4. **Operational flow chart of the LoRa-enabled point-of-care system.**

drivers include low cost, ease of use, long shelf life, and evolving specificity and sensitivity [88]. Such tests enable the detection of biological molecules, or biomarkers, which are associated with both pathological and non-pathological medical conditions. Typical sample sources for point-of-care testing include patient urine, blood or saliva, and diagnostic specificity is typically engendered through chemical reactions.

Historically strips have been visually assessed 'by eye' for visible color change on the strip to deliver qualitative or semi-quantitative detection of biomarkers using a chemical dye reaction or accumulation of colored nanoparticles on a specific region of the test strip. However, if some form of electronic detection is used then some tests are capable of delivering fully quantitative diagnostic measurements.

A number of different electronic reading techniques have been implemented, ranging from charge-coupled device (CCD) imaging [89], reflectance, or transmission [90] mode analysis of test strips. For reliable point-of-care use, the challenge is to produce a robust portable device capable of fully quantitative analysis and preferably allowing dissemination of results. We report here on the initial use of the diagnostic reader to obtain qualitative data from disposable test 'keys'. The patient sample is added to these keys before being placed into the reader. The key comprises the biomarker detection strip positioned within a custom ABS plastic housing, designed for secure engagement and optical alignment into the diagnostic reader. A transmission-based optical sensing technique is utilized for measurement using an illumination light emitting diode (LED) oriented geometrically opposite a photodetector. Upon insertion of the test key the optical path between illumination LED and photodetector is occluded, with biomarker detection resulting in a color change that alters strip absorbance and hence the number of photons detected by the photodetector. To achieve maximal sensitivity the illumination LED and photodetector were both optically matched both to each other, and selected to give maximum response over the expected range of color change reactions exhibited by the urinalysis dipstick.

This was achieved by using a scanning spectrophotometer to generate absorption spectra for 'post-reaction' test strips. Absorption maxima were identified for strips exhibiting a 'positive reaction' (assessed by visual comparison of the reacted strip with a urinalysis color chart); these were then used as criteria for selecting the wavelength of the Transmission LED and photodetector (data not shown).

C. URINARY TRACT INFECTIONS AS A USER CASE

UTIs are typically caused by either Escherichia coli bacteria or associated with abnormalities of the urinary tract that disable the patient's natural defences leading to tissue injury; symptoms of urinary tract infections include painful urination, frequent urination, or loin pain [91]. It is estimated that 35% of women suffer urinary tract infection symptoms at some time in their life. Although UTI symptoms and treatment are straightforward, for some, particularly the elderly, symptoms may not be clear enough to immediately diagnose. A wait of several days between obtaining a urine sample and receiving laboratory results can delay treatment potentially leading to more serious health implications. Point-of-care urinalysis dipsticks are readily available and have been shown to be useful to rapidly identify or rule out infection. Measurement from these strips is semi-quantitative and somewhat subjective since it involves manual alignment of the wetted strip with a color chart for visual assessment of the intensity of color development.

In this trial a 'test key' containing two sample windows holds a Urinalysis Strip (Suresign Professional, CIGA Healthcare, Ballymena, Northern Ireland). The strip possesses several biomarker detection zones, two of which are sensitive to either urinary NIT (produced by the action of Gram-negative bacteria in the urine), or urinary Leucocyte esterase (LE) (an enzyme released from granulocytic white blood cells as part of the innate immune response). A single

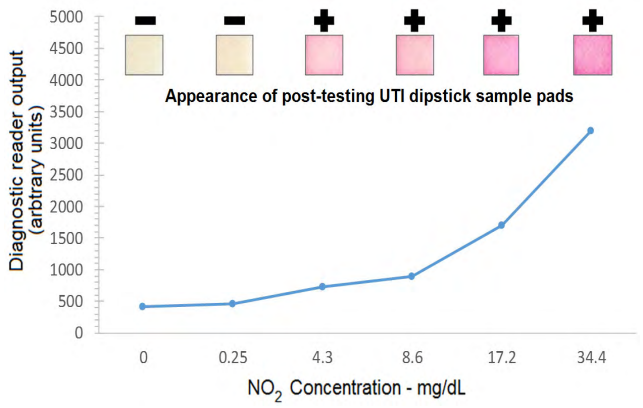

FIGURE 5. Diagnostic reader response to increasing NO_2 concentration.

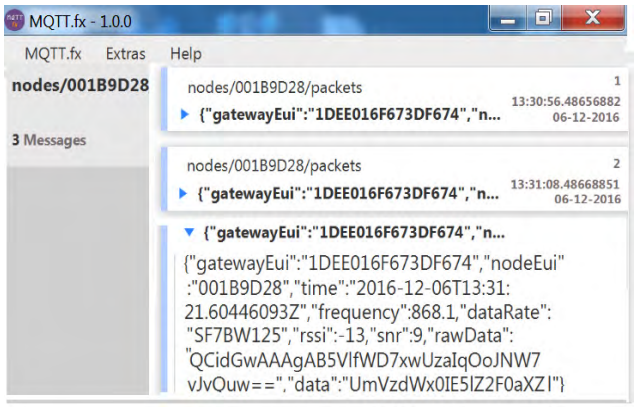

FIGURE 6. Screenshot of MQTT broker used to observe server data.

drop of urine is placed into each sample window on the test key where it is rapidly absorbed into the paper-based detection substrate for reaction with the test zones. Pathological urine will cause formation of strip-localized colored dye compounds within 2 minutes, leading to a change in optical absorbance.

As the diagnostic biosensor was to be used as a first level screening test, it was necessary for it to be able to discriminate between healthy and pathological urine samples. This was achieved through the creation of a diagnostic threshold - an experimentally derived sensor output value, against which unknown samples could be assessed. To maximize sensitivity, a diagnosis of UTI was made only when a sample was positive for both NIT and LEU activity.

A series of samples were prepared to enable correlation of diagnostic reader's sensor output with urinalysis results. These samples contained increasing concentrations of either NIT or LEU reactive compounds, chosen to span the healthy to pathological concentration range. An example using NIT-containing solutions (Sigma 72587 - NIT standard solution) is shown in Fig. 5, where a concentration-dependent variation in diagnostic reader sensor output can be observed. Similar work was performed to establish the sensor response to the LEU reactive portion of the test strip (results not show).

Following urinalysis by diagnostic reader the strips were immediately subject to visual scoring using either the relevant NIT or LEU portion of the manufacturer-provided urinalysis color comparison chart. Examples of post-test NIT test pad regions are shown in Fig. 5. Samples were scored as either positive or negative (+ or −), as indicated above each sample pad insert on Fig. 5.

By selecting a diagnostic reader sensor output value from within the range between the highest negative and lowest positive sample (as established through visual scoring using the urinalysis color chart) it was possible to set the 'diagnostic threshold'. This is indicated by the horizontal cover line on Fig. 5. Any unknown sample yielding a diagnostic reader sensor output value greater than the threshold values for both NIT and LE was considered to be UTI positive. The robustness of this threshold approach was assessed independently using a set of blinded positive and negative patient samples, achieving a 92.7% correct rate.

The UTI detection threshold was input to the companion Android 'app' and transmitted, together with test duration and type, to the diagnostic reader via BLE. The diagnostic reader then analyzes any inserted UTI test key according to these transmitted parameters. A positive diagnosis from this diagnostic strip requires that absorbance measurements from both NIT and LE regions of the strip be correlated. The photodiode output signal was therefore continuously communicated to the companion app, upon completion of the test the final photodiode outputs for both detection regions are compared against the thresholds. A single test result (positive or negative) was then communicated to the secure server using LoRa, the results of which were observed via the MQTT broker (Fig. 6). A series of both control and known pathological urine samples were used to demonstrate the diagnostic performance of the diagnostic reader system.

III. TEST PLAN AND METHODOLOGY

The tests were conducted over 3 sites (one rural, one urban, and one suburban) and at 3 selected locations around each of the sites (see Fig. 7 - 9 for details.). For each of these locations two test strips giving a "RESULT_POSITIVE" and "RESULT_NEGATIVE" outcome were used. This totaled 18 tests in all. All tests were conducted in the bathroom of each property due to the nature of the test.

For location 1 (Fig. 7) the base-station/gateway was located in Coleraine, UK with GPS co-ordinates N55° 6′ 47.21″, W6° 39′ 16.22″. The antenna mounted on outside mounting at 2.3 m above the ground. The location is an area of dense forestry (mostly 15m+ Ash trees) which itself is surrounded by fields and hills, thus highlighting operation in difficult rural terrain. The diagnostic system was tested at the 3 locations marked on the map. Test site 1.1 was a concrete block residential dwelling (detached bungalow) of 1970s construction to the East of the base-station with GPS co-ordinates N55° 6′ 16.08″, W6° 34′ 10.28″. Test site 1.2 was a two story farm house of 1990s construction surrounded by fields to the West of the base-station with co-ordinates N55° 6′ 1.72″,

IEEE Journal of Translational Engineering in Health and Medicine

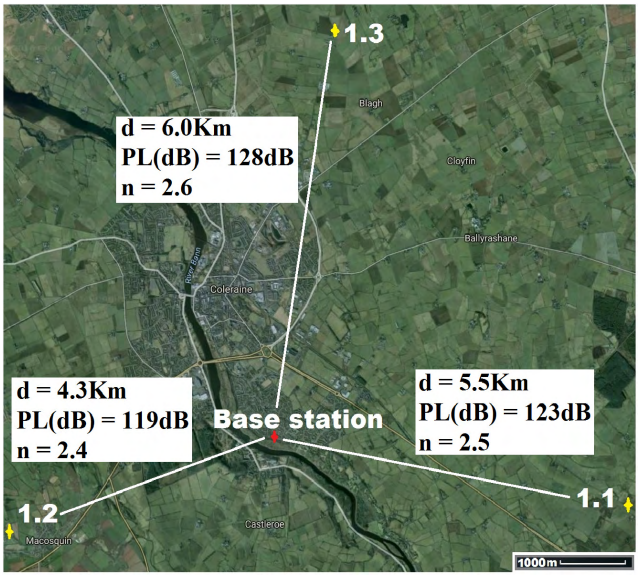

FIGURE 7. Test area 1 (Rural location).

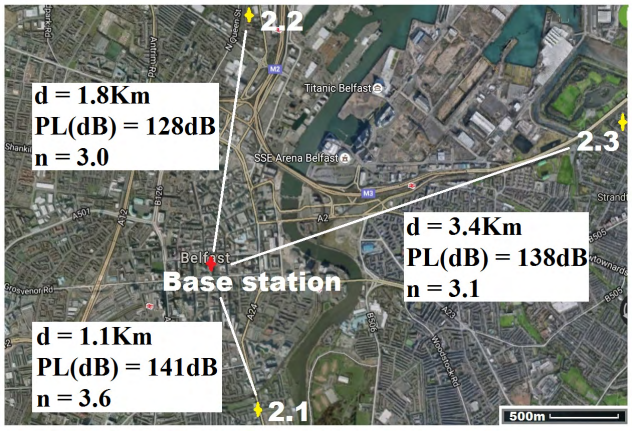

FIGURE 8. Test area 2 (City location).

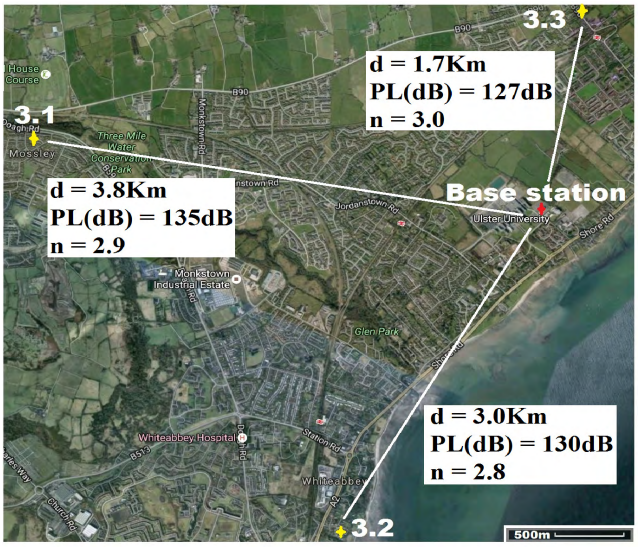

FIGURE 9. Test area 3 (Suburban location).

W6° 43′ 5.03″. Test site 1.3 was a two story semi-detached house in a rural farming area (1960s) and to the North of the base-station with co-ordinates N55° 10′ 0.26″, W6° 38′ 21.63″.

For location 2 (Fig. 8) the gateway was located at the heart of the city of Belfast with GPS co-ordinates N54° 35′ 47.79″, W5° 55′ 54.31″. The antenna mounted on outside mounting at 20 m above the ground. The location is a densely populated urban area surrounded by heavy industry (including shipping) and emphasizes operation in a busy modern city. The diagnostic system was tested at the 3 locations marked on the map (Fig. 8). Test site 2.1 was a three story brick town house of 1930s construction to the South of the base-station with GPS co-ordinates N54° 35′ 15.12″, W5° 55′ 27.02″. Test site 2.2 was a retirement fold (sheltered housing community) consisting of single story apartments 1990s construction to the North of the base-station with GPS co-ordinates N54° 36′ 44.50″, W5° 55′ 31.04″. Test site 2.3 was a two story large detached house in an established residential area erected in the 1950s and to the East of the base-station with GPS co-ordinates N54° 36′ 23.95″, W5° 52′ 56.61″.

For location 3 (Fig. 9) the gateway was located at UU, BT37 with GPS co-ordinates N54° 41′ 15.72″, W5° 52′ 41.24″. The antenna mounted on outside mounting at 6 m above the ground. The location is a large university campus area surrounded by suburban housing. This location examines operation in the leafy suburbs. The diagnostic system was tested at the 3 locations marked on the map (Fig. 9). Test site 3.1 was a concrete block detached bungalow dwelling of early 1970s construction to the West of the base-station with co-ordinates N54° 41′ 35.26″, W5° 56′ 11.98″. Test site 3.2 was a large detached two story house of mid 1990s construction in are large housing development to the South of the base-station with co-ordinates N54° 39′ 54.92″, W5° 54′ 5.95″. Test site 3.3 was a two story detached house in an established residential area erected in the 1950s and to the North of the base-station with GPS co-ordinates N54° 42′ 10.63″, W5° 52′ 33.59″.

IV. RESULTS AND DISCUSSION

The measurements were recorded as per the protocol above. The secure server recorded the outcome of the test, the received signal level power (in dBm), the sequence order of the test, and the time and date of the recording. For clinical purposes this would allow the identification of the patient and subsequent automated Electronic Health Record (EHR) input.

A. DIAGNOSTIC SYSTEM TEST RESULTS

Results presented in Table 2 clearly indicate that the new diagnostic system operated correctly during all the tests, giving correct results based on the particular inserted

TABLE 2. Urinary tract infection trial results for the nine specified test sites.

	Location 1 (Rural) (N55º 6' 47.21", W6 º 39' 16.22")		
Test site	**1.1**	**1.2**	**1.3**
GPS co-ordinates	N55º 6' 16.08", W6º 34' 10.28"	N55º 6' 1.72", W6º 43' 5.03"	N55º 10' 0.26", W6º 38' 21.63"
Device/base-station separation (Km)	5.5	4.3	6.0
Result Positive	Confirmed	Confirmed	Confirmed
Result Negative	Confirmed	Confirmed	Confirmed

	Location 2 (City) (N54º 35' 47.79", W5 º 55' 54.31")		
Test site	**2.1**	**2.2**	**2.3**
GPS co-ordinates	N54º 35' 15.12", W5º 55' 27.02"	N54º 36' 44.50", W5 º 55' 31.04"	N54º 36' 23.95", W5º 52' 56.61"
Device/base-station separation (Km)	1.1	1.8	3.4
Result Positive	Confirmed	Confirmed	Confirmed
Result Negative	Confirmed	Confirmed	Confirmed

	Location 3 (Suburban) (N54º 41' 15.72", W5 º 52' 41.24")		
Test site	**3.1**	**3.2**	**3.3**
GPS co-ordinates	N54º 41' 35.26", W5 º 56' 11.98"	N54º 39' 54.92", W5º 54' 5.95"	N54º 42' 10.63", W5º 52' 33.59"
Device/base-station separation (Km)	3.8	3.0	1.7
Result Positive	Confirmed	Confirmed	Confirmed
Result Negative	Confirmed	Confirmed	Confirmed

UTI test strip. This was confirmed through visual assessment of test strip with the urinalysis chart provided by the dipstick manufacturer. The advantage of the electronic analysis of strips is that each strip is held in the correct orientation for analysis under defined lighting conditions within the reader. The reader analysis is based, not on human interpretation, but on comparison with an experimentally defined threshold. This removes the subjective nature of conventional point-of-care dipstick urinalysis which requires users to make a judgement based on multiple colour intensity comparisons, and correctly interpret results.

Although the content of this report concerns UTI diagnosis the diagnostic methodology for this reader is substantially the same for pathologies including bacterial pneumonia, anaemia and HIV. Laboratory and field trials for such conditions have been conducted using the diagnostic reader as part of the Qualcomm Tricorder XPRIZE competition.

Results were transmitted via the LoRa network to the secure server, and presented correct data (including test results, date and time, received radio power level, signal to noise ratio, gateway identification, transmission frequency, and packet number) onto the servers for observation and confirmation. The system was designed specifically for use by a patient and assumed the patient has little or no IT ability. The system is simple to use and should something untoward occur during testing the patient user can simply cycle the power on the unit and start again. However the new LoRa-enable diagnostic reader operated correctly during all the community UTI trials.

For each test activity the system determined and transmitted the correct results based on the inserted UTI test strip. The signal from the diagnostic system connected with the nearest LoRa gateway and the gateway routed the results and other test-related information in the correct manner to the specified secure server. Using the MQTT (example in Fig. 6) the server record was observed and verified as accurate in terms of test results, the transmitted date and time, the gateway identification listed, the transmission frequency (automatically selected by the LoRa radio system), packet number, and received radio power levels at the gateway.

IEEE Journal of Translational Engineering in Health and Medicine

Thus it was confirmed that all locations sent back correct data to the secure server. These results across various regions and locations within those regions clearly demonstrate the opportunity to realize secure remote healthcare which requires no subscription fees, SIM cards, access to the 3G/4G mobile network, Wi-Fi access, or an operational landline in the property.

B. ANALYSIS OF THE COMMUNICATIONS CHANNEL

If the remote healthcare solution is required to operate in all environments, terrain, and scenarios it is important to understand the quality of the communications channel. The remote healthcare system is targeted for deployment in domiciliary care environments; therefore we present the following long range network parameters to determine signal robustness and quality of service; received signal strength level, effective path losses between device and base station, signal-noise ratio, and the path loss exponent. The received signal strength level (RSSI) at the base-station from the transmitting diagnostic system allows us to determine the quality of the secure radio link based on the separation distance and the terrain between diagnostic system and base-station site. The signal-noise ratio (SNR) also acts as an indicator of link quality with respect to the radio channel's environmental parameters. It is the ratio of the power of the information signal and the power of incoherent background noise, mathematically expressed as;

$$SNR = \frac{P_{signal}}{P_{noise}} \tag{1}$$

where P is average power for each expression when the power of both signal and noise is considered over the same bandwidth of interest. Furthermore each of the values are often expressed in decibels;

$$P_{signal(dB)} = 10\log_{10}(P_{signal}) \tag{2}$$

$$P_{noise(dB)} = 10\log_{10}(P_{noise}) \tag{3}$$

And subsequently the SNR can be expressed as decibels;

$$SNR_{(dB)} = P_{signal(dB)} - P_{noise(dB)} \tag{4}$$

Additionally, an understanding of the radio link quality can be determined by modelling the path losses using the well-recognized Log-distance path loss model. The average large-scale path loss for each transmitter-receiver separation can be suitably expressed as a function of distance using a path loss exponent, $\boldsymbol{n}$, which is dependent on carrier frequency, environment, obstructions, etc. The Log-distance path loss is given by:

$$\overline{PL}(d) = PL(d_0) + 10n\log_{10}(d/d_0) \tag{5}$$

where $\boldsymbol{n}$ is the path loss exponent indicating the rate at which the path loss increases with distance, $\boldsymbol{d_0}$ is the close-in reference distance which is determined from measurement close to the transmitter, and $\boldsymbol{d}$ is the transmitter-receiver separation distance. The path loss exponent ($\boldsymbol{n}$) can thus be calculated;

$$n = \overline{PL}(d) - PL(d_0)/10\log_{10}(d/d_0) \tag{6}$$

The signal losses are caused by natural free space loss which occurs as the signal travels through space, as well as additional losses of which the most prominent for these scenarios would be absorption losses into surrounding objects (buildings, trees, etc.) in the communication path.

Table 3 presents details of the long range network parameters for the tests to help understand the quality and reliability of this medical network. It is not sufficient to declare that it worked, but crucial to understand the parameters by which it worked to ensure a more rigorous comprehension of operation. Such parameters including the aforementioned RSSI, path loss, SNR, and path loss exponent allow the apprehension of how well the wireless portion of the medical diagnostic system worked during the tests and to appreciate what environmental or operational factors compromise the quality of the communications channel and inform as to what the limitations of such systems may be.

Results in table 3 highlight the received signal strength of the transmitted signal were each apposite values that reflect a dependable system that can operate inside houses without issues of signal loss or data-link failure (lead-lined houses would cause issues but these would be a rarity and issues are circumvented by taking the system beside an open window). The best RSSI value (highest received power) was observed in test 1.2 and the worst in 2.1; this is a reflection on the distances travelled and the environment through which the signal traversed from the diagnostic system.

Signal to noise ratio (SNR) for each test is presented and the "−" sign indicates that the signal power is below the noise floor threshold. This is one of the key advantages of the LoRa technology and allows data to be received below power levels where signals are normally lost in the background noise (such as is the case with the cell phone network). Minus value SNR were observed for 6 of the 9 test cases. The highest SNR was recorded from test 1.2 and the lowest for test 2.1; again an indicator that the wireless transmission aspect of the system is less robust in highly dense urban areas (although still perfectly functional) and best in open rural areas. Additionally the path loss exponent ($\boldsymbol{n}$) for each test is presented with the lowest value observed in test 1.2 where the propagating data signal had few obstacles in its path towards the base station, whereas 2.1 had the highest exponent where the signal travelled through a dense urban environment with multiple signal absorbers, reflectors and scatterers. In each environment the values of $\boldsymbol{n}$ measured are in keeping with [92].

Fig. 7-9 (and Table 3) also detail the path losses experienced by the signal carrying the transmitted results back to the base station. They clearly highlight that regardless of the operational environment for the medical diagnostic tester the technology offers a robust method of long range secure data transmission. Only test results from location 2.1 to the city center base station gave any cause for concern as this amount of path loss is close to the maximum working limits. However this can be easily improved by better positioned base stations with larger antennas, as well as more than one base station

TABLE 3. Urinary tract infection trial details for the long range wireless transmission of test results to the secure server.

	Location 1 (Rural) (N55° 6' 47.21", W6 ° 39' 16.22")		
Test site	**1.1**	**1.2**	**1.3**
Device/base-station separation (Km)	5.5	4.3	6.0
Frequency channel (MHz)	868.5	868.3	868.5
RSSI (dBm)	-109	-105	-114
Path loss (dB)	123	119	128
SNR (dB)	1.1	2.0	-4.2
n	2.5	2.4	2.6

	Location 2 (City) (N54° 35' 47.79", W5 ° 55' 54.31")		
Test site	**2.1**	**2.2**	**2.3**
Device/base-station separation (Km)	1.1	1.8	3.4
Frequency channel (MHz)	868.1	868.3	868.3
RSSI (dBm)	-127	-114	-124
Path loss (dB)	141	128	138
SNR (dB)	-17.2	-6.8	-12.5
n	3.6	3.0	3.1

	Location 3 (Suburban) (N54° 41' 15.72", W5 ° 52' 41.24")		
Test site	**3.1**	**3.2**	**3.3**
Device/base-station separation (Km)	3.8	3.0	1.7
Frequency channel (MHz)	868.1	868.1	868.5
RSSI (dBm)	-121	-116	-113
Path loss (dB)	135	130	127
SNR (dB)	-16.0	-12.5	1.7
n	2.9	2.8	3.0

covering an entire city; should such a system be deployed then choice locations would be selected and a typical number of 3 base stations would be used to allow additional features such as triangulation and elimination of bad reception in density packed environments (such as New York).

C. OTHER SIGNIFICANT FINDINGS

IoT servers typically employ User Datagram Protocol (UDP) port numbers such as 1700, but in many large organizations (commercial/private networks) such port numbers are blocked by the corporate firewall. This causes network set-up problems as without access to the particular IP address it is not possible to set up two-way communications between the base-station and the back-end server. For the LoRa network this can be circumvented by using one way communications with the base-station sending information out (with no receive acknowledgement from the back-end server). The other key IoT technology, Sigfox, uses a business model more akin to the cell phone network where large companies develop the infrastructure, therefore corporate firewall and port issues are less of a difficulty. However, coverage in remotest areas cannot be solved by the end user (as it can for LoRa), instead requiring network development by provider.

Battery life for our testing purposes was not a particular issue and in practical operation the system would typically be used a few times a day for a period of a few weeks. If longer term monitoring is required then emerging energy harvesting solutions such as photovoltaic harvesting (solar power) could be employed and/or the processing and LEDs of the diagnostic reader could be optimized for lower power to ensure longer operation from a single battery. Alternatively a charging station could be used or a mains power supply as such a device is typically used in the same place (kitchen or bedroom), however this may affect the potential

IEEE Journal of Translational Engineering in Health and Medicine

mobility of the user during activities of daily living and is thus much less desirable. Energy requirements are 200mW when the LEDs are on and 120mW when off. Conducting the UTI test takes on average approximately 225 seconds which mean that the system can be used some 400 times on one 9v battery (Duracell - 550mAh). To date the system is not optimized power consumption; further development can only increase the number of tests achievable per battery.

A final point of note regards the operation of the system within our biomedical research and development facility. The building was constructed with a metal mesh to act as a Faraday shield against electromagnetic interference; this makes a barrier against signals getting in and out of the building. While the chances of operating the system within such a building arrangement would be rare it should still be noted that transmission distances are considerably reduced. However as the system is truly portable it is considered that the test could be conducted with an open door, or indeed conducted in a porch, conservatory, or simply outside.

V. CONCLUSION

A significant step in realizing the next generation of remote healthcare systems has been taken. The 868 MHz LoRaWAN-enabled personalized healthcare device demonstrated its potential with the UTI test results being correctly diagnosed and transmitted to a remote secure cloud server in each case. The validity of a medical diagnostics system enabled with IoT technology and deployed in residential settings has been investigated and proven to yield robust telemetry results to the attending clinician at the hospital or medical center via the LoRa network. The tests ranged over a distance of 1.1 – 6.0 Km and displayed radio path losses from 119 – 141 dB. Furthermore, all tests conducted were correctly and robustly received at the base station and relayed to the secure server for inspection. The UTI test strips were visually inspected for correct diagnosis based on color change and verified as 100% correct. Results from both urban and rural environments highlight that such a system has the capacity to be deployed in any part of a country. Such technology can foreseeably make a genuine impact on how patients with chronic conditions are monitored, and using this developed solution as a platform it is possible to enable any monitoring or medical device with the same remote capability. As the Lora network infrastructure becomes deployed throughout Europe, USA, and beyond there is a true opportunity to meet the needs of the global ageing population.

The next step is to characterize the sensitivity and specificity of the system against clinically approved standards, as well as to put the system in the hands of typical target user groups to understand the strengths and limitations of using such a system. This will allow us to evaluate the feasibility of real-world data collection and redevelop unfavorable aspects of the technology before considering clinical trials.

We have thus presented a diagnostics system suitable for use by a patient who has been sent home from hospital or who suffers from a chronic condition. It allows them to perform daily tests regardless of whether they live in an urban or rural area, have a mobile signal in their area, and have a broadband connection or even a landline in their home. We have proven that the Internet of Things is a promising solution for chronic illness monitoring in the community and as a portable solution for travelling homecare workers, midwives, etc.

REFERENCES

[1] Gartner. (2015). *21 Billion IoT Devices to Invade By 2020*. [Online]. Available: http://www.informationweek.com/mobile/mobile-devices/gartner-21-billion-iot-devices-to-invade-by-2020/d/d-id/1323081

[2] Research and Markets. (2016). *Global Forecast to 2021*. [Online]. Available: http://www.researchandmarkets.com/research/gsjxb5/internet_of

[3] Active Telecoms. (2016). *Chinese Manufacturers Tipped to Spend $127b Annually on IoT*. [Online]. Available: http://activetelecoms.com/news/internet-of-things/chinese-manufacturers-tipped-to-spend-127b-annually-on-iot

[4] D.-G. Zhang, X.-D. Song, X. Wang, and Y.-Y. Ma, "Extended AODV routing method based on distributed minimum transmission (DMT) for WSN," *Intl. J. Electron. Commun.*, vol. 69, no. 1, pp. 371–381, 2015.

[5] D. Zhang, G. Li, K. Zheng, X. Ming, and Z. H. Pan, "An energy-balanced routing method based on forward-aware factor for wireless sensor networks," *IEEE Trans. Ind. Inform.*, vol. 10, no. 1, pp. 766–773, Feb. 2014.

[6] S. Liu and T. Zhang, "Novel unequal clustering routing protocol considering energy balancing based on network partition & distance for mobile education," *J. Netw. Comput. Appl.*, vol. 88, pp. 1–9, Jun. 2017.

[7] D.-G. Zhang, X. Wang, X.-D. Song, T. Zhang, and Y.-N. Zhu "A new clustering routing method based on PECE for WSN," *EURASIP J. Wireless Commun. Netw.*, vol. 162, pp. 1–13, Jun. 2015.

[8] D. Zhang, C. P. Zhao, Y.-P. Liang, and Z.-J. Liu, "A new medium access control protocol based on perceived data reliability and spatial correlation in wireless sensor network," *Comput. Elect. Eng.*, vol. 38, no. 3, pp. 694–702, 2012.

[9] D.-G. Zhang, Y.-N. Zhu, C.-P. Zhao, and W.-B. Dai, "A new constructing approach for a weighted topology of wireless sensor networks based on local-world theory for the Internet of Things," *Comput. Math. Apps.*, vol. 64, no. 5, pp. 1044–1055, 2012.

[10] D.-G. Zhang, K. Zheng, D. Zhao, X.-D. Song, and X. Wang, "Novel quick start (QS) method for optimization of TCP," *Wireless Netw.*, vol. 22, no. 1, pp. 211–222, 2016.

[11] D.-G. Zhang, S. Zhou, and Y.-M. Tang, "A low duty cycle efficient MAC protocol based on self-adaption and predictive strategy," in *Mobile Networks and Applications*. New York, NY, USA: Springer, May 2017, doi: https://doi.org/10.1007/s11036-017-0878-x

[12] Z. Ma, D. Zhang, S. Liu, J. Song, and Y. Hou, "A novel compressive sensing method based on SVD sparse random measurement matrix in wireless sensor network," *Eng. Comput.*, vol. 33, no. 8, pp. 2448–2462, 2016.

[13] D.-G. Zhang and Y.-P. Liang, "A kind of novel method of service-aware computing for uncertain mobile applications," *Math. Comput. Model.*, vol. 57, nos. 3–4, pp. 344–356, 2013.

[14] D.-G. Zhang, K. Zheng, T. Zhang, and X. Wang, "A novel multicast routing method with minimum transmission for WSN of cloud computing service," *Soft Comput.*, vol. 19, no. 7, pp. 1817–1827, 2015.

[15] D.-G. Zhang, X.-D. Song, X. Wang, K. Li, W.-B. Li, and Z. Ma, "New agent-based proactive migration method and system for big data environment (BDE)," *Eng. Comput.*, vol. 32, no. 8, pp. 2443–2466, 2015.

[16] D.-G. Zhang, "A new approach and system for attentive mobile learning based on seamless migration," *Appl. Intell.*, vol. 36, no. 1, pp. 75–89, 2012.

[17] D. Zhang, X. Wang, X. Song, and D. Zhao, "A novel approach to mapped correlation of ID for RFID anti-collision," *IEEE Trans. Services Comput.*, vol. 7, no. 4, pp. 741–748, Oct. 2014.

[18] S. M. R. Islam, D. Kwak, M. D. H. Kabir, M. Hossain, and K.-S. Kwak, "The Internet of Things for health care: A comprehensive survey," *IEEE Access*, vol. 3, pp. 678–708, Jun. 2015.

[19] D.-G. Zhang, X. Wang, and X. Song, "New medical image fusion approach with coding based on SCD in wireless sensor network," *J Elect. Eng. Technol.*, vol. 10, no. 6, pp. 2384–2392, 2015.

[20] D. Zhang, X. Kang, and J. Wang, "A novel image de-noising method based on spherical coordinates system," *EURASIP J. Adv. Signal Process.*, vol. 110, pp. 1–10, May 2012.

[21] D.-G. Zhang, W. B. Li, S. Liu, and X.-D. Zhang "Novel fusion computing method for bio-medical image of WSN based on spherical coordinate," *J. Vibroeng.*, vol. 18, no. 1, pp. 522–538, 2016.

[22] Z. Ma, D.-G. Zhang, J. Chen, and Y.-X. Hou "Shadow detection of moving objects based on multisource information in Internet of things," *J. Experim. Theor. Artif. Intell.*, vol. 29, no. 3, pp. 649–661, 2017.

[23] X. Zhang and X.-D. Zhang, "Design and implementation of embedded un-interruptible power supply system (EUPSS) for Web-based mobile application," *Enterprise Inf. Syst.*, vol. 6, no. 4, pp. 473–489, 2012.

[24] V. Sai and M. H. Mickle, "Low power 8051-MISA-based remote execution unit architecture for IoT and RFID applications," *Int. J. Circuits Archit. Des.*, vol. 1, no. 1, pp. 4–19, 2013.

[25] V. Sai and M. H. Mickle, "Exploring energy efficient architectures in passive wireless nodes for IoT applications," *IEEE Circuits Syst. Mag.*, vol. 14, no. 2, pp. 48–54, 2nd Quart., 2014.

[26] K. Laubhan, K. Talaat, S. Riehl, M. S. Aman, A. Abdelgawad, and K. Yelamarthi, "A low-power IoT framework: From sensors to the cloud," in *Proc. IEEE Int. Conf. Electro Inf. Technol.*, Grand Forks, ND, USA, May 2016, pp. 0648–0652.

[27] V. Sai and M. H. Mickle, "Low-power smart passive REU for industrial IoT applications," *Int. J. Circuits Archit. Des.*, vol. 2, no. 2, pp. 105–117, 2016.

[28] P. A. Catherwood, D. Branagh, D. D. Finlay, and J. A. D. McLaughlin, "Future directions of power sources for ambulatory ECG monitors," in *Proc. Comput. Cardiol. Conf. (CinC)*, Nice, France, Sep. 2015, pp. 405–408.

[29] P. A. Catherwood and W. G. Scanlon, "Off-body UWB channel characterisation within a hospital ward environment," *Int. J. Ultra Wideband Commun. Syst.*, vol. 1, no. 4, pp. 263–272, 2010.

[30] N. Sornin, M. Luis, T. Eirich, T. Kramp, and O. Hersent, "LoRaWAN specification version 1.0.1," LoRa Alliance, San Ramon, CA, USA, Tech. Rep. V1.0.1 Draft 3, Oct. 2015.

[31] ReadWrite News. (2016). *Orange Goes LoRa to Connect French Smart Cities*. [Online]. Available: http://readwrite.com/2016/06/17/orange-picks-lora-protocol-smart-city-france-pt4/

[32] *Things Network*. Accessed: May 2017. [Online]. Available: www.thethingsnetwork.org

[33] M. T. Buyukakkaslar, M. A. Erturk, M. A. Aydin, and L. Vollero, "LoRaWAN as an e-health communication technology," in *Proc. IEEE 41st Annu. Comput. Softw. Appl. Conf. (COMPSAC)*, Turin, Italy, Jul. 2017, pp. 310–313.

[34] J. Petäjäjärvi, K. Mikhaylov, M. Hämäläinen, and J. Iinatti, "Evaluation of LoRa LPWAN technology for remote health and wellbeing monitoring," in *Proc. 10th Int. Symp. Med. Inf. Commun. Technol. (ISMICT)*, Worcester, MA, USA, Mar. 2016, pp. 1–5.

[35] A. Mdhaffar, T. Chaari, K. Larbi, M. Jmaiel, and B. Freisleben, "IoT-based health monitoring via LoRaWAN," in *Proc. IEEE EUROCON 17th Int. Conf. Smart Technol.*, Ohrid, Macedonia, Jul. 2017, pp. 519–524.

[36] L. Krupka, L. Vojtech, and M. Neruda, "The issue of LPWAN technology coexistence in IoT environment," in *Proc. Int. Conf. Mechatron., Mechatron.*, Prague, Czech Republic, Dec. 2016, pp. 1–8.

[37] *Bluetooth Core Specification Version 4.2*, 2nd ed., Bluetooth SIG, Kirkland, WA, USA, Dec. 2014.

[38] *Bluetooth Core Specification Version 5.0*, 6th ed., Bluetooth SIG, Kirkland, WA, USA, Dec. 2016.

[39] *ZigBee Specification Version Release 20*, document 053474r20, ZigBee Alliance, Sep. 2012.

[40] *Requirements Related to Technical Performance for IMT-Advanced Radio Interfaces*, document Rep. M.2134, ITU, Geneva, Switzerland, 2008.

[41] X. Ge, S. Tu, G. Mao, and C. X. Wang, "5G ultra-dense cellular networks," *IEEE Trans. Wireless Commun.*, vol. 23, no. 1, pp. 72–79, Feb. 2016.

[42] *LTE; Evolved Universal Terrestrial Radio Access (E-UTRA); User Equipment (UE) Radio Transmission and Reception*, document TS 36.101 version 13.6.1 Release 13, ETSI, Mar. 2017.

[43] *Short-Range Narrow-Band Digital Radiocommunication Transceivers*, document Rec. G.9959, ITU, Geneva, Switzerland, 2015.

[44] *IEEE Standard for Information Technology—Specific Requirements—Part II*, IEEE Standard 802.11-2016, Dec. 2016, pp.1-3534.

[45] *Information Technology-Radio Frequency Identification for Item Management—Part 3: Parameters for Air Interface Communications at 13.56 MHz*, document ISO/IEC 18000-3:2010, International Organization for Standardization, Geneva, Switzerland, 2010.

[46] *Cellular System Support for Ultra-Low Complexity and Low Throughput Internet of Things (CIoT)*, document TR 45.820 V13.1.0 Release 13, 3GPP, Nov. 2015.

[47] *United Nations, Department of Economic and Social Affairs, Population Division (2013)*, document ST/ESA/SER.A/348, World Population Ageing, 2013.

[48] A. Steventon *et al.*, *Effect of Telehealth on Use of Secondary Care and Mortality: Findings From the Whole System Demonstrator Cluster Randomised Trial*, document 344:e3874, BMJ, 2012.

[49] J. Henriques *et al.*, "Prediction of heart failure decompensation events by trend analysis of telemonitoring data," *IEEE J. Biomed. Health Inform.*, vol. 19, no. 5, pp. 1757–1769, Sep. 2015.

[50] G. Kang, "Wireless eHealth (WeHealth)—From concept to practice," in *Proc. IEEE 14th Int. Conf. e-Health Netw., Appl. Services*, Beijing, China, Oct. 2012, pp. 375–378.

[51] S. K. Datta, C. Bonnet, A. Gyrard, R. P. F. da Costa, and K. Boudaoud, "Applying Internet of Things for personalized healthcare in smart homes," in *Proc. 24th Wireless Opt. Commun. Conf.*, Taipei, Taiwan, Oct. 2015, pp. 164–169.

[52] K. R. Darshan and K. R. Anandakumar, "A comprehensive review on usage of Internet of Things (IoT) in healthcare system," in *Proc. Int. Conf. Emerg. Res. Electron., Comput. Sci. Technol.*, Mandya, India, Dec. 2015, pp. 132–136.

[53] D. Azariadi, V. Tsoutsouras, S. Xydis, and D. Soudris, "ECG signal analysis and arrhythmia detection on IoT wearable medical devices," in *Proc. 5th Int. Conf. Modern Circuits Syst. Technol.*, Thessaloniki, Greece, May 2016, pp. 1–4.

[54] E. Spanò, S. Di Pascoli, and G. Iannaccone, "Low-power wearable ECG monitoring system for multiple-patient remote monitoring," *IEEE Sensors J.*, vol. 16, no. 13, pp. 5452–5462, Jul. 2016.

[55] C. F. Pasluosta, H. Gassner, J. Winkler, J. Klucken, and B. M. Eskofier, "An emerging era in the management of Parkinson's disease: Wearable technologies and the Internet of Things," *IEEE J. Biomed. Health Inform.*, vol. 19, no. 6, pp. 1873–1881, Nov. 2015.

[56] D. Niyato, X. Lu, P. Wang, D. I. Kim, and Z. Han, "Economics of Internet of Things: An information market approach," *IEEE Wireless Commun.*, vol. 23, no. 4, pp. 136–145, Aug. 2016.

[57] Y. Zhang, L. Sun, H. Song, and X. Cao, "Ubiquitous WSN for healthcare: Recent advances and future prospects," *IEEE Internet Things J.*, vol. 1, no. 4, pp. 311–318, Aug. 2014.

[58] L. Lizzi, F. Ferrero, P. Monin, C. Danchesi, and S. Boudaud, "Design of miniature antennas for IoT applications," in *Proc. IEEE 6th Int. Conf. Commun. Electron.*, Ha Long, Vietnam, Jul. 2016, pp. 234–237.

[59] L. Catarinucci *et al.*, "An IoT-aware architecture for smart healthcare systems," *IEEE Internet Things J.*, vol. 2, no. 6, pp. 515–526, Dec. 2015.

[60] M. Rossi, A. Rizzi, L. Lorenzelli, and D. Brunelli, "Remote rehabilitation monitoring with an IoT-enabled embedded system for precise progress tracking," in *Proc. IEEE Int. Conf. Electron., Circuits Syst.*, Monte Carlo, Monaco, Dec. 2016, pp. 384–387.

[61] A. M. Ghosh, D. Halder, and S. K. A. Hossain, "Remote health monitoring system through IoT," in *Proc. 5th Int. Conf. Inform., Electron. Vis.*, Dhaka, Bangladesh, May 2016, pp. 921–926.

[62] M. Lauridsen, I. Z. Kovacs, P. Mogensen, M. Sorensen, and S. Holst, "Coverage and capacity analysis of LTE-M and NB-IoT in a rural area," in *Proc. IEEE 84th Veh. Technol. Conf.*, Montreal, QC, Canada, Sep. 2016, pp. 1–5.

[63] P. Neumann, J. Montavont, and T. Noël, "Indoor deployment of low-power wide area networks (LPWAN): A LoRaWAN case study," in *Proc. IEEE 12th Int. Conf. Wireless Mobile Comput., Netw. Commun.*, New York, NY, USA, Oct. 2016, pp. 1–8.

[64] A. J. Wixted, P. Kinnaird, H. Larijani, A. Tait, A. Ahmadinia, and N. Strachan, "Evaluation of LoRa and LoRaWAN for wireless sensor networks," in *Proc. IEEE Sensors*, Orlando, FL, USA, Nov. 2016, pp. 1–3.

[65] U. Raza, P. Kulkarni, and M. Sooriyabandara, "Low power wide area networks: An overview," *IEEE Commun. Surveys Tuts.*, vol. 19, no. 2, pp. 855–873, 2nd Quart., 2017.

[66] P. Raj and A. C. Raman, *The Internet of Things: Enabling Technologies, Platforms, and Use Cases*. Boca Raton, FL, USA: CRC Press, 2017.

[67] M. Kuroda and M. Fukahori, "Affordable M2M enabled e-health using standard ban technology," in *Proc. IEEE Healthcare Innov. Conf.*, Oct. 2014, pp. 276–279.

[68] C. C. Y. Poon, B. P. L. Lo, M. R. Yuce, A. Alomainy, and Y. Hao, "Body sensor networks: In the era of big data and beyond," *IEEE Rev. Biomed. Eng.*, vol. 8, pp. 4–16, 2015.

[69] H. Lee, H. Cho, and H.-J. Yoo, "A 33 μW/node duty cycle controlled HBC transceiver system for medical BAN with 64 sensor nodes," in *Proc. IEEE Custom Integr. Circuits Conf.*, Sep. 2014, pp. 1–8.
[70] T. Douseki and A. Tanaka, "Self-powered wireless disposable sensor for welfare application," in *Proc. 35th Annu. Int. Conf. IEEE Eng. Med. Biol. Soc.*, Jul. 2013, pp. 1664–1667.
[71] N. N. Dhalwani *et al.*, "Long terms trends of multimorbidity and association with physical activity in older English population," *Int. J. Behav. Nutrition Phys. Act.*, vol. 13, no. 1, p. 8, 2016.
[72] C. Imison, S. Castle-Clarke, R. Watson, and N. Edwards, "Delivering the benefits of digital health care," Nuffield Trust, London, U.K., Res. Rep., 2016, pp. 5–6.
[73] HSJ. (2015). *NHS England: Digital Plans 'Could Save $10bn'*. [Online]. Available: http://www.hsj.co.uk/news/nhs-england-digital-plans-could-save-10bn/5086921.article
[74] C. Barbosa and T. Dong, "Modelling and design of a capacitive touch sensor for urinary tract infection detection at the point-of-care," in *Proc. 36th Annu. Int. Conf. IEEE Eng. Med. Biol. Soc.*, Chicago, IL, USA, Aug. 2014, pp. 4995–4998.
[75] P. Béland, O. Krupin, and P. Berini, "Selective detection of bacteria in urine with a LRSPP waveguide biosensor," in *Proc. Photon. North*, Ottawa, ON, Canada, Jun. 2015, p. 1.
[76] K. Hadjigeorgiou, E. Kastanos, A. Kyriakides, and C. Pitris, "Point-of-care diagnosis of urinary tract infection (UTI) using surface enhanced Raman spectroscopy (SERS)," in *Proc. IEEE 12th Int. Conf. Bioinform. Bioeng. (BIBE)*, Larnaca, Cyprus, Nov. 2012, pp. 333–337.
[77] M. Ra, M. S. Muhammad, C. Lim, S. Han, C. Jung, and W.-Y. Kim, "Smartphone-based point-of-care urinalysis under variable illumination," *IEEE J. Transl. Eng. Health Med.*, vol. 6, pp. 1–11, 2018.
[78] R. Sarno, K. Christian, R. V. H. Ginardi, and D. Sunaryono, "Examination results of leukocytes and nitrites in the early detection of urinary tract infection," in *Proc. Int. Conf. Comput., Control, Inform. Appl. (IC3INA)*, Bandung, Indonesia, Oct. 2015, pp. 45–49.
[79] C. Chen, Y. Wu, and T. Dong, "Dipsticks integrated on smart diapers for colorimetric analysis of urinary tract infections in the field," in *Proc. 16th Int. Conf. Mechatron.-Mechatron.*, Brno, Czech Republic, Dec. 2014, pp. 423–427.
[80] S. Feng, T. Dong, and Z. Yang, "Detection of urinary tract infections on lab-on-chip device by measuring photons emitted from ATP bioluminescence," in *Proc. 36th Annu. Int. Conf. IEEE Eng. Med. Biol. Soc.*, Chicago, IL, USA, Aug. 2014, pp. 3114–3117.
[81] S. Feng, L. E. Roseng, and T. Dong, "Quantitative detection of Escherichia coli and measurement of urinary tract infection diagnosis possibility by use of a portable, handheld sensor," in *Proc. IEEE Int. Symp. Med. Meas. Appl. (MeMeA)*, Turin, Italy, May 2015, pp. 586–589.
[82] M. N. Hasan, A. Fraiwan, J. A. Little, and U. A. Gurkan, "A low-cost, mass-producible point-of-care platform for diagnosing hemoglobin disorders," in *Proc. IEEE Healthcare Innov. Point Care Technol. (HI-POCT)*, Bethesda, MD, USA, Nov. 2017, pp. 164–167.
[83] A. Ukil, S. Bandyoapdhyay, C. Puri, and A. Pal, "IoT healthcare analytics: The importance of anomaly detection," in *Proc. IEEE 30th Int. Conf. Adv. Inf. Netw. Appl.*, Crans-Montana, Switzerland, Mar. 2016, pp. 994–997.
[84] *Ideetron Website*. Accessed: May 2017. [Online]. Available: www.ideetron.nl
[85] Tricorder XPrize. (2016). *Intelesens-Scanadu*. [Online]. Available: http://tricorder.xprize.org/teams/scanadu
[86] Grand View Research, "Blood pressure monitoring devices market analysis by product (sphygmomanometers, automated blood pressure monitor, transducers, ambulatory blood pressure monitor, instrument & accessories, blood pressure cuffs, bladders, bulbs,valves), and segment forecasts to 2022," Grand View Research, San Francisco, CA, USA, Res. Rep. 978-1-68038-586-1, Jul. 2016, pp. 1–60.
[87] Grand View Research, "Diabetes devices market size to reach $35.5 billion by 2024," Grand View Research, San Francisco, CA, USA, Res. Rep. 978-1-68038-873-2, May 2016, pp. 1–85.
[88] J. Hu *et al.*, "Advances in paper-based point-of-care diagnostics," *Biosensors Bioelectron.*, vol. 54, pp. 585–597, Apr. 2014.
[89] C. Gui, K. Wang, C. Li, X. Dai, and D. Cui, "A CCD-based reader combined with CdS quantum dot-labeled lateral flow strips for ultrasensitive quantitative detection of CagA," *Nanoscale Res. Lett.*, vol. 9, no. 1, p. 57, 2014.
[90] A. K. Ellerbee *et al.*, "Quantifying colorimetric assays in paper-based microfluidic devices by measuring the transmission of light through paper," *Anal. Chem.*, vol. 81, no. 20, pp. 8447–8452, 2009.
[91] J. B. L. Lee and G. H. Neild, "Urinary tract infection," *Medicine*, vol. 35, no. 8, pp. 423–428, 2007.
[92] R. G. Vaughan and J. B. Anderson, *Channels, Propagation and Antennas for Mobile Communications*. London, U.K.: IET, 2017.